RSC Advances




ROYAL SOCIETY OF CHEMISTRY

www.rsc.org/advances

RSC Advances

RSC Publishing

ARTICLE

# The assembly and photoelectronic property of reduced graphene oxide/porphyrin/phthalocyanine composite films

Cite this: DOI: 10.1039/x0xx00000x

Received 00th March 2015,
Accepted 00th March 2015

DOI: 10.1039/x0xx00000x

www.rsc.org/

Meijuan Zhang,[a] Bing Yuan,[a] Shi-zhao Kang,[a] Lixia Qin,[a] Guodong Li[b] and Xiangqing Li*[a]

By layer–by–layer self–assembly method, reduced graphene oxide (RGO)–based composite films with highly photoelectronic activity were assembled with 5, 10, 15, 20–tetrakis (p–N, N, N–trimethylanilinium) porphyrin tetraiodide (TAPPI) and copper sulfophthalocyanine (CuTsPc) as the co–sensitizers. The π–π interaction and electrostatic interaction were the main driving forces of the assembly. The linear dependence of the absorption on the layer numbers of the films demonstrated the formation of the ordered films. In the composite film, an efficient photoinduced electron transfer can take place as evidenced by fluorescence spectra. Furthermore, the photoelectronic response for the RGO/TAPPI/CuTsPc film was higher than that of the RGO/TAPPI film, the RGO/CuTsPc film or the TAPPI/CuTsPc film. The complemental absorption spectra of TAPPI and CuTsPc and the quick transfer of photoproduced electrons could be the main reasons for the enhanced photoelectronic response in the RGO/TAPPI/CuTsPc film.

## 1. Introduction

Graphene, a monolayer of two–dimensional $sp^2$–hybridized carbon atoms that are covalently organized as a honeycomb structure, has attracted tremendous attention owing to the unique combination of electrical, thermal, mechanical, and chemical properties.[1–4] Based on the special structure and properties, graphene shows potential applications in sensors, energy storage devices, transparent conducting electrodes and catalysis.[5–8] However, perspective applications of graphene based materials would be limited due to the solubility and/or processability of the graphene. Compared to graphene, graphene oxide (GO) bears hydroxyl and epoxide functional groups on their basal planes, in addition to carbonyl and carboxyl groups located at the sheet edges. The availability of several types of oxygen–containing functional groups allows GO to easily be functionalized and interacts with a wide range of organic and inorganic materials, which is important to graphene processing.[9]

Covalent or noncovalent functionalization of graphene with various dyes has been considered to be important in biological sensors,[10] photovoltaic device[11] and photocatalyst.[12] Porphyrins, a class of multifunctional π–conjugated molecules, have been used to modify graphene sheets. Wu et al. prepared a novel photocatalytic system based on porphyrin and graphene, which not only showed a higher conversion rate of $CH_4$, but also could convert $CO_2$ to acetylene under visible light irradiation.[12] They also found that meso-tetra(4-carboxyphenyl)porphine can stabilize reduced graphene oxide and detect dopamine with higher sensitivity and selectivity.[13] In addition, the graphene/porphyrin composites have also shown other promising applications such as photoelectrochemical cells,[14] optical probe[15] and photocatalytic hydrogen production.[16] As another important dye, metallophthalocyanines are also of great interest due to their excellent electronic properties and potential applications in some fields such as electrical devices, solar cells and biosensors.[10,17,18] Currently, several research groups have explored the phthalocyanine functionalized graphenes[19–23] and their applications in sensor[10] and electrocatalysis.[24]

How the graphene based composites can be reasonably incorporated into a photoelectric device, especially if effective use requires precise optimization of optical path length and crystal–thickness, remains unclear. An attractive alternative would be to directly synthesize the graphene based composite as the supported thin films. Layer–by–layer (LbL) assembly technique provides a simple and versatile method of preparing graphene–based composite films.[25] This strategy makes it possible to control the film thickness, composition, morphology and functionality on a nanoscale level, and the films assembled have the potential applications.[26–28] Cui et al. developed a novel nitrite sensor based on multilayer films containing graphene and cobalt phthalocyanine.[29] Zhang et al. prepared a glucose biosensor by immobilizing glucose oxidase on graphene/copper phthalocyanine ultrathin films.[10] Sun et al. assembled the multiple–bilayered RGO–porphyrin films and studied the

photoelectrochemical properties of the films.[14] Though the graphene films sensitized by porphyrin or phthalocyanine alone show a good performance, the performance of films, especially photoelectronic performance, is still low due to the insufficient use of light energy. Now, it is found that the mixed (phthalocyaninato) (porphyrinato) europium triple–decker could be acted as a balanced–mobility, ambipolar organic thin film transistor.[30] Its properties would be further improved if the electrons can be transferred more quickly.

Herein, with reduced graphene oxide (RGO) as the carrier of electron transfer, 5, 10, 15, 20–tetrakis (p–N, N, N–trimethylanilinium) porphyrin tetraiodide (TAPPI) and copper sulfophthalocyanine (CuTsPc) as the cosensitizers, a new type of composite films composed of TAPPI, CuTsPc and RGO is fabricated by LbL method followed by chemical reduction. The assembly and the photoelectrochemical property of the films are investigated.

## 2. Experimental

### 2.1. Materials

Graphite powder with an average size of 30 μm and purity of > 95% was obtained from Shanghai Chemical Reagent Company. The GO was prepared by a modified Hummers method.[31] TAPPI was synthesized and purified according to the Ref..[32] CuTsPc and polydiallyldimethylammonium chloride (PDDA) were purchased from Aldrich and used without further purification. The other reagents (A.R.) came from Shanghai Chemical Reagent Company and were used as received. Double distilled water was used throughout the experiments.

### 2.2. Treatment of the substrates

First, the substrates (quartz glasses or Si slices) were cleaned by sonication in ethanol, acetone, chloroform and double distilled water for 20 min, respectively, and then dried with air flow. The cleaned substrate was sonicated for 1 h in a piranha solution (the volume ratio of concentrated $H_2SO_4$ to $H_2O_2$ solution is 7: 3), and placed in the piranha solution for one more hour. After that, the substrate was rinsed with double distilled water and acetone, respectively, and dried with air flow. For the fluorine–doped tin oxide (FTO) glass, it was treated by sonication in a saturated KOH alcohol solution for 2 min. After that, the FTO glass was rinsed with double distilled water and acetone, respectively, and dried with air flow.

### 2.3. Fabrication of the (RGO/TAPPI/CuTsPc/TAPPI)$_n$ films

PDDA is a polyelectrolyte with rich positive charges. First, the clean substrate (The substrate treated as 2.2 is with negative charges) was immersed into PDDA aqueous solution (0.05 wt%) overnight. Then, the substrate was taken out, rinsed with double distilled water, and dried with air flow. Subsequently, PDDA monolayer was adhered on the substrate via electrostatic interaction.

After that, the PDDA–treated substrate with positive charges was soaked into a GO aqueous solution (1 mg mL$^{-1}$). After 20 min, the substrate was taken out and rinsed with double distilled water in order to remove the physically absorbed GO. Then, it was dried, and alternately immersed into TAPPI and CuTsPc solution, respectively, and treated just like the procedure of GO assembled on the substrate. By this means, one unit of the GO/TAPPI/CuTsPc/TAPPI film was assembled on the substrate. As shown in Fig. 1, repeated the procedure, the multilayer films could be prepared. After the (GO/TAPPI/ CuTsPc/TAPPI)$_n$ composite films were reduced at 40 °C for 36 h with the help of hydrazine hydrate, the brown film became brownish black. Referenced to the literature,[33] it was deduced that the (RGO/TAPPI/CuTsPc/TAPPI)$_n$ films were achieved.

### 2.4. Characterization

UV–visible spectra were recorded with a model U–3900/U–3900H spectrophotometer (Japan). Fluorescence spectra were obtained using a Hitachi F–4600 fluorescence spectrofluorophotometer (Japan). AFM images were taken on an Agilent Technologies N9605A atomic force microscope with tapping mode (USA). Electrochemical experiments were performed with a CHI 660B electrochemical analyzer (Chenhua Co., Shanghai, China). Amperometric I–t curves, cyclic voltammograms (CV) and electrochemical impedance spectra (EIS) were measured with a three–electrode cell, including the FTO glass coated with the film as the working electrode, a Ag/AgCl (saturated KCl) electrode as the reference electrode and a Pt wire as the counter electrode. PBS solution (mixture of $NaH_2PO_4$ and $Na_2HPO_4$) containing 0.9% NaCl was used as the electrolyte. The light source was a 150 W xenon lamp (absorption region: 200 nm–1800 nm). The distance between light source and the working electrode was 7 cm. The air in the solution was removed by purging nitrogen for 15 min. Electrochemical impedance spectra (EIS) were tested with the potentiostatic mode in the range of 10 Hz to $10^6$ Hz, and the bias potential was open circuit voltage. The amplitude was 5 mV.

## 3. Results and discussion

The (GO/TAPPI/CuTsPc/TAPPI)$_n$ films were fabricated mainly via two procedures: (1) assembly of the (GO/TAPPI/CuTsPc/TAPPI)$_n$ films by using a LbL method (Fig. 1); (2) chemical reduction of the films with hydrazine hydrate.

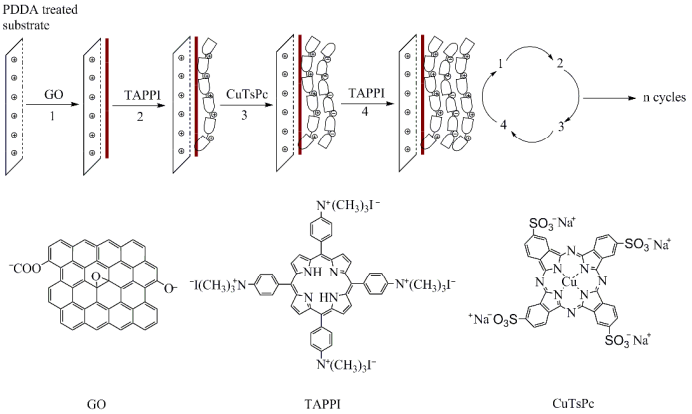


**Fig. 1.** Schematic representation of the assembly process of (GO/TAPPI/CuTsPc/TAPPI)$_n$ films.

It is known that the GO prepared by Hummers method[31] is negatively charged. As shown in the Fig.1, TAPPI is positively charged, and CuTsPc is negatively charged. So the electrostatic interaction and the π–π interaction among GO, TAPPI and CuTsPc are the driving force for the assembly of (GO/TAPPI/CuTsPc/TAPPI)$_n$ films.

In order to enhance the stability of the films, the strong interaction between the substrate and GO is vital. So a photo–inert PDDA monolayer with rich positive charges was first grown on the substrate. Followed by the increase of the layer numbers, it is found that the color of the (GO/TAPPI/CuTsPc/TAPPI)$_n$ films gradually deepens, and becomes nigger–brown when the layer number is 6 (Fig. 2A). Whether the (GO/CuTsPc/TAPPI)$_n$ films were uniformly



 

assembled or not, it was further evidenced by the UV–vis spectra (Fig. 2B). It is observed that the absorbance of the films at 232 nm and 424 nm is gradually enhanced followed by increasing the layer numbers. The absorbance at about 232 nm is attributed to the π–π* transition of aromatic C = C vibration coming from GO (228 nm) and CuTsPc (226 nm). The absorbance at 424 nm is attributed to the Soret band of TAPPI, and the minor adsorption peak around 520 nm is attributed to Q band of the TAPPI. The two absorbance are red–shifted compared with those of the TAPPI solution (not shown here), indicating that the TAPPI J–aggregates have been formed in the film.[34] In addition, a broad band in the range of 520 nm to 750 nm can be observed. It is attributed to Q bands of the TAPPI and CuTsPc, mainly CuTsPc. The absorption also increases with the layer number just like those at 232 nm and at 424 nm. Obviously, the absorption region of the GO is widened after assembling with TAPPI and CuTsPc, which is profitable for the utilization of the light. Moreover, the relationship between the absorbance (at 232 nm and 424 nm) and the layer number is almost linear (Fig. 2B, inset), and correlation coefficient is 0.99683 and 0.99994, respectively. It provides a powerful evidence for the layer–by–layer assembly of the films.

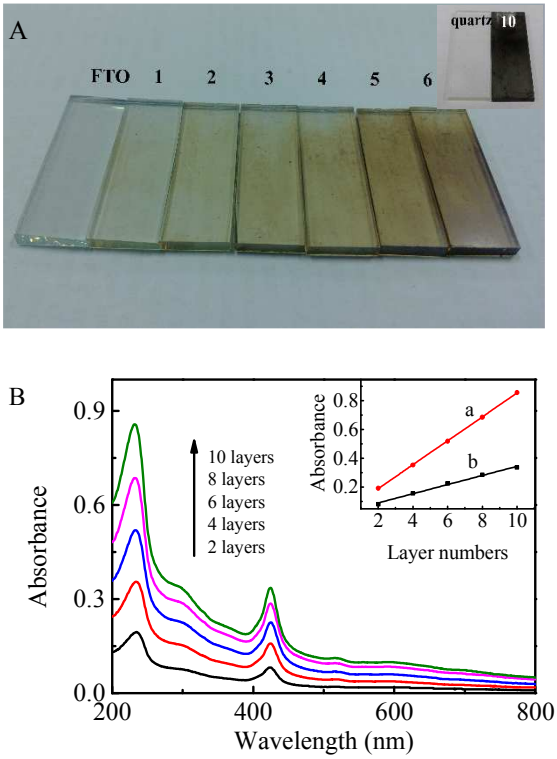


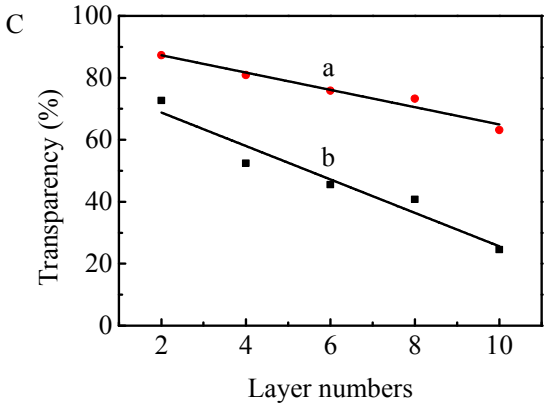


**Fig. 2.** (A) The digital image of the $(GO/TAPPI/CuTsPc/TAPPI)_n$ films assembled on FTO substrates (n = 1, 2, 3, 4, 5, 6) and the inset is the digital image of the $(RGO/TAPPI/CuTsPc/TAPPI)_{10}$ films assembled on FTO substrate; (B) UV−vis absorption spectra of the $(GO/TAPPI/CuTsPc/TAPPI)_n$ films (n = 2, 4, 6, 8, 10). The inset is the dependence of the absorbance at 232 nm (a) and 424 nm (b) on layer numbers, respectively; (C) the dependence of the transparency of the film (before (a) and after (b) being reduced) on layer numbers.

After the $(GO/TAPPI/CuTsPc/TAPPI)_n$ films were reduced with the help of hydrazine hydrate, the films became dark (Fig. 2A, inset), suggesting that the GO in the films had been reduced to RGO.[35] Moreover, the transparency decreases with increasing the layer numbers of the film (Fig. 2C), which could prevent the photos from being captured efficiently.

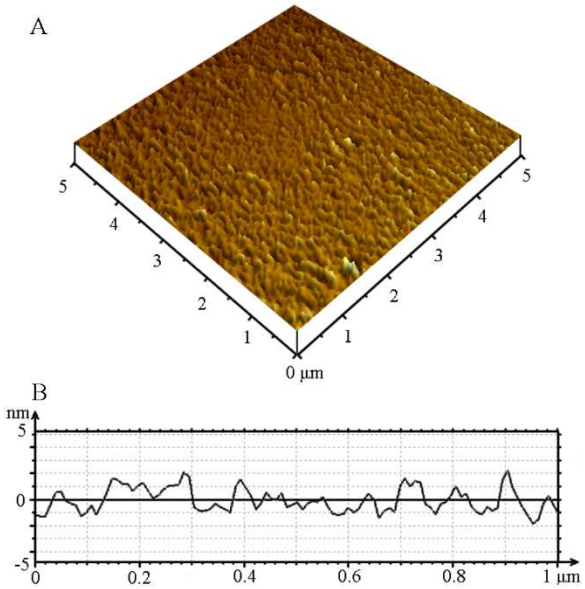


**Fig. 3.** The AFM image (A) and the line profile (B) of the GO/TAPPI/CuTsPc monolayer film.

As shown in the AFM image of the GO/TAPPI/CuTsPc monolayer film (Fig. 3), the surface of the film is uniform. The result of line profile reveals the thickness of the GO/TAPPI/CuTsPc monolayer film is about 4 nm.

The interaction among RGO, TAPPI and CuTsPc is investigated by fluorescence spectroscopy. As displayed in Fig. 4, two emission peaks for the TAPPI are observed at 655 and 712 nm, respectively.

In contrast, after introducing the CuTsPc, the fluorescence for the TAPPI is partly quenched, and the fluorescence is further quenched when introducing RGO into the TAPPI/CuTsPc. It is indicated that an efficient photoinduced electron transfer can occurred from TAPPI to CuTsPc and RGO.

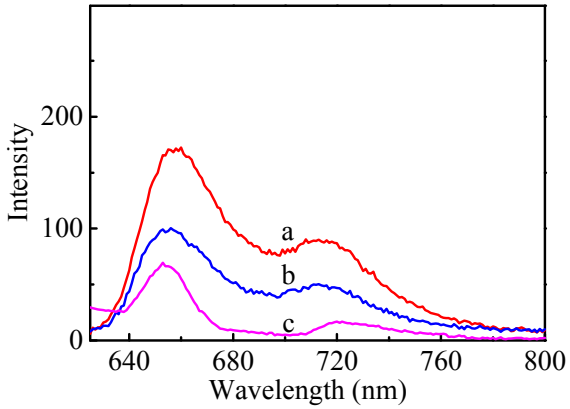


**Fig. 4.** Fluorescence spectra of the TAPPI film (a), the TAPPI/CuTsPc film (b) and the RGO/TAPPI/CuTsPc film (c). $\lambda_{ex}$ = 423 nm.

Electrochemical impedance spectra (EIS) of the RGO/TAPPI/CuTsPc and the GO/TAPPI/CuTsPc electrodes are measured. As shown in Fig. 5, the diameter of the semicircle for the RGO/TAPPI/CuTsPc electrode is obviously smaller than that of the GO/TAPPI/CuTsPc electrode. It is demonstrated that the resistance of the RGO/TAPPI/CuTsPc electrode is lower than that of the GO/TAPPI/CuTsPc electrode. It is attributed to the reduced surface defects in the RGO/TAPPI/CuTsPc film. So that electron transfer in the GO/TAPPI/CuTsPc film can be quickened after being treated with hydrazine hydrate.

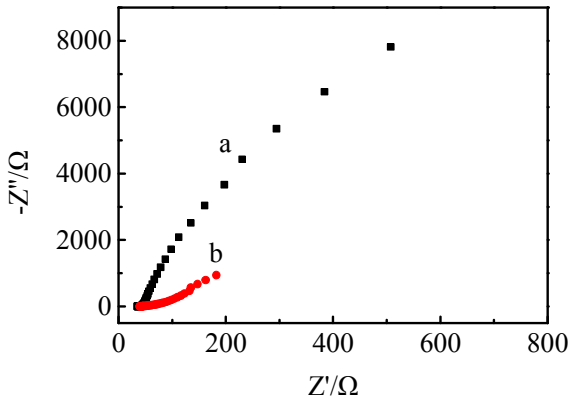


**Fig. 5.** Nyquist plots of EIS under illumination for the GO/TAPPI/CuTsPc electrode (a) and the RGO/TAPPI/CuTsPc electrode (b).

In order to demonstrate the roles of TAPPI and CuTsPc in the RGO/TAPPI/CuTsPc composite film, cyclic voltammetry (CV) spectra of the RGO/TAPPI/CuTsPc film, RGO/CuTsPc film and RGO/TAPPI film are measured (Fig. 6A). It can be seen that, the higher photocurrent can be observed for the RGO/TAPPI/CuTsPc film. It is known that, the Soret band and Q bands of the CuTsPc are in the range of 200–250 nm and 550–750 nm, respectively. The Soret band and Q bands of the TAPPI are in the range of 400–420 nm and 500–650 nm, respectively (not shown here). Obviously, absorbance of the TAPPI and the CuTsPc is complementary. Therefore, both the CuTsPc and the TAPPI are the suitable co–sensitizers of the RGO, and TAPPI and CuTsPc co-sensitized RGO make use of light more efficiently compared with single TAPPI or CuTsPc sensitized RGO, which makes a positive contribution to the enhanced photocurrent in the RGO/TAPPI/CuTsPc film.

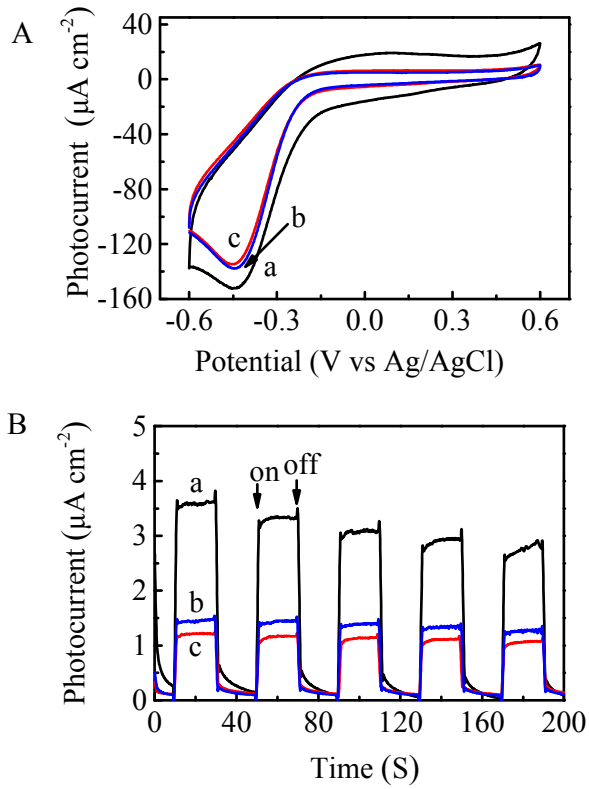


**Fig. 6.** (A) CV spectra of various films and (B) I–t curves under illumination. (a) RGO/TAPPI/CuTsPc, (b) RGO/CuTsPc and (c) RGO/TAPPI films.

Furthermore, photoelectrochemical responses of the films are investigated. Clearly, the photocurrents of three electrodes are stable and the responses are prompt. After five on–off light cycles, the photocurrent of the RGO/TAPPI/CuTsPc is slightly decreased. However it is still higher than those of the RGO/CuTsPc and RGO/TAPPI. When the bias potential is open circuit voltage, and the amplitude is 5 mV, the photocurrent generated from RGO/TAPPI/CuTsPc, RGO/CuTsPc and RGO/TAPPI films is 3.5 μA, 1.5 μA and 1.2 μA, respectively. Obviously, both the TAPPI and CuTsPc make a positive contribution to the enhanced photocurrent in the RGO/TAPPI/CuTsPc film.

In order to demonstrate the role of RGO in the film, CV spectra of the RGO/TAPPI/CuTsPc film, the RGO film and the CuTsPc/TAPPI film are also measured. As a semiconductor material, RGO can be excited after absorbing the light. When the photo–produced electrons are transferred to FTO electrode, the photocurrent is observed in the film electrode of the RGO (Fig. 7b). After introducing RGO into the CuTsPc/TAPPI film, the photocurrent of the TAPPI/CuTsPc films is obviously increased. As reported in the literatures,[10,14,16] graphene could act as the electron accepter and the carrier to transport electrons away from the holes. According to the

result in Fig. 7A, it is concluded that the RGO in the composite film can effectively facilitate the dissociation of the photoproduced excitons of the CuTsPc/TAPPI, and further transport the electrons to the FTO electrode, so the photocurrent of the CuTsPc/TAPPI film is increased. In addition, after introducing CuTsPc/TAPPI, the photocurrent of the RGO film is also enhanced. The photocurrent is in the order of RGO/TAPPI/CuTsPc > RGO > CuTsPc/TAPPI (Fig. 7B). Obviously, both the RGO and the CuTsPc/TAPPI provide positive contribution for the anodic photocurrent generation of the RGO/TAPPI/CuTsPc composite film. Thus, compared with the other films, the RGO/TAPPI/CuTsPc composite film could act as a more efficient photo–anode material. In addition, the RGO/TAPPI/CuTsPc film electrode pre-treated with a photo–inert PDDA monolayer is stable. The surface of the film is hardly changed except the slightly decreased photocurrent after being recycled for over eight times. The photocurrent of RGO/TAPPI/CuTsPc decays a little in Fig. 6–7 compared with the other films, which might be due to the higher recombination of electrons and holes in the RGO/TAPPI/CuTsPc film than in the other films.[36]

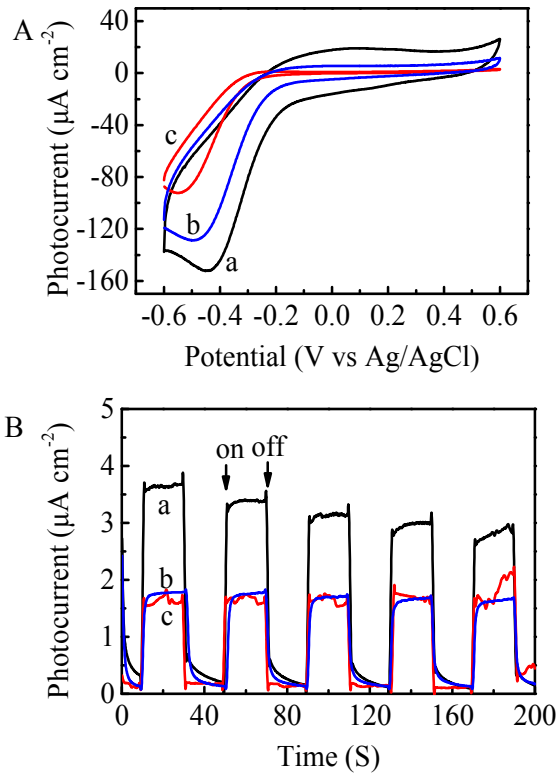


**Fig. 7.** (A) CV spectra of various films and (B) I–t curves under illumination. (a) The RGO/TAPPI/CuTsPc, (b) RGO and (c) CuTsPc/TAPPI films.

In addition, the relationship between the photocurrent density of the FTO/(RGO/TAPPI/CuTsPc/TAPPI)$_n$ films electrode and the layer numbers of the films is investigated (The (RGO/TAPPI/CuTsPc/TAPPI)$_n$ films were not assembled directly by the RGO/TAPPI/CuTsPc film used in Fig. 6-7. That is, the microenvironment of the two films and the FTO substrates are different). As shown in Fig. 8, the generated photocurrent varies with the layer numbers of the films. When the layer number is lower than 4, the photocurrent of the films enhances followed with the increased layer number, which demonstrates the uniform assembly of RGO, TAPPI and CuTsPc on the FTO substrate, and the separation efficiency of electron/hole pairs in the film is positive. However, the photocurrent decreases when the layer number of the films is beyond 4. It could be attributed to the following reasons: (i) the transparency decreased with increasing the layer numbers of the film (Fig. 2C), which could prevent the photos from being captured efficiently; (ii) the increased resistance generated in the electron transport across the layers offset the increased light–harvesting when the films became relatively thicker;[29] (iii) the harvesting of photoexcited electrons vertically through the thicker film was inefficient.[34]

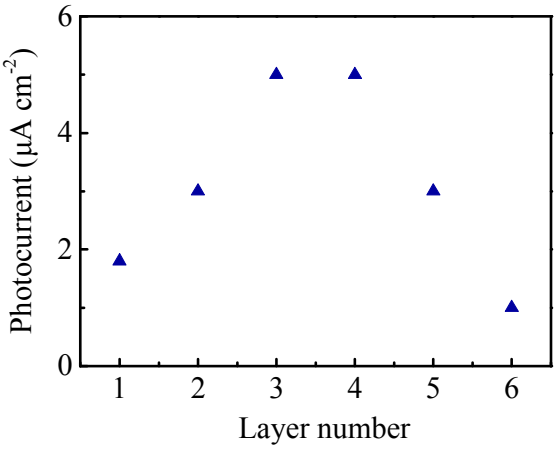


**Fig. 8.** Dependence of photocurrent of the (RGO/TAPPI/CuTsPc/TAPPI)$_n$ films on the layer numbers of the films.

## 4. Conclusions

In summary, the (RGO/TAPPI/CuTsPc/TAPPI)$_n$ composite films were uniformly assembled onto various substrates though the layer–by–layer self–assembly method. The (RGO/TAPPI/CuTsPc/TAPPI)$_n$ films exhibited a higher redox activity and significant anodic photocurrent generation, indicating excellent electron transfer and efficient absorption of light in the CuTsPc and TAPPI co–sensitized RGO films. This study would provide important information for developing potential photoelectric conversion and storage devices as well as photocatalytic molecular devices.

## Acknowledgements

This work was financially supported by the National Natural Science Foundation of China (Grant Nos. 21301118, 21305092 and 21371070), and Innovation Program of Shanghai Municipal Education Commission (No. 15ZZ096).

## Notes and references

[a].School of Chemical and Environmental Engineering, Shanghai Institute of Technology, 100 Haiquan Road, Shanghai 201418, China. *E-mail address*: xqli@sit.edu.cn

[b] State Key Laboratory of Inorganic Synthesis and Preparative Chemistry, College of Chemistry, Jilin University, Changchun 130012, China.

1 J. H. Chen, C. Jang, S. Xiao, M. Ishigami and M. S. Fuhrer, *Nat. Nanotechnol.*, 2008, 3, 206–209.
2 A. A. Balandin, S. Ghosh, W. Bao, I. Calizo, D. Teweldebrhan, F. Miao and C. N. Lau, *Nano Lett*., 2008, 8, 902–907.
3 C. Lee, X. Wei, J. W. Kysar and J. Hone, *Science*, 2008, 321, 385–388.
4 K. S. Novoselov, Z. Jiang, Y. Zhang, S. V. Morozov, H. L. Stormer, U. Zeitler, J. C. Maan, G. S. Boebinger, P. Kim and A. K. Geim, *Science*, 2007, 315, 1379.
5 L. Zhan , Y. Zhang, Q. L. Zeng, Z. D. Liu and C. Z. Huang, *J. Colloid Interface Sci.*, 2014, 426, 293–299.
6 L. B. Ma, X. P. Shen, Z. Y. Ji, X. Q. Cai, G. X. Zhu and K. M. Chen, *J. Colloid Interface Sci.* 2015, 440, 211–218.
7 Y. Zhu, Z. Sun, Z. Yan, Z. Jin and J. M. Tour, *ACS Nano*, 2011, 5, 6472–6479.
8 G. Williams, B. Seger and P. V. Kamat, *ACS Nano*, 2008, 2, 1487–1491.
9 Y. Y. Liang, D. Q. Wu, X. L. Feng and K. Mullen, *Adv. Mater.*, 2009, 21, 1679–1683.
10 Y. Q. Zhang, Y. J. Fan, L. Cheng, L. L. Fan, Z. Y. Wang, J. P. Zhong, L. N. Wu, X. C. Shen and Z. J. Shi, *Electrochim. Acta*, 2013, 104, 178–184.
11 L. Kavan, J. H. Yum and M. Grätzel, *Nano Lett.*, 2011, 11, 5501–5506.
12 T. S. Wu, L. Y. Zou, D. X. Han, F. H. Li, Q. X. Zhang and L. Niu, *Green Chem.*, 2014, 16, 2142–2146.
13 L. Wu, L. Y. Feng, J. S. Ren and X. G. Qu, *Biosens. Bioelectron.*, 2012, 34, 57–62.
14 J. H. Sun, D. L. Meng, S. D. Jiang, G. F. Wu, S. K. Yan, J. X. Geng and Y. Huang, *J. Mater. Chem.*, 2012, 22, 18879–18886.
15 Y. X. Xu, L. Zhao, H. Bai, W. J. Hong, C. Li and G. Q. Shi, *J. Am. Chem. Soc.*, 2009, 131, 13490–13497.
16 M. S. Zhu, Z. Li, B. Xiao, Y. T. Lu, Y. K. Du, P. Yang and X. M. Wang, *ACS Appl. Mater. Interfaces*, 2013, 5, 1732–1740.
17 J. Bartelmess, B. Ballesteros, G. de la Torre, D. Kiessling, S. Campidelli, M. Prato, T. Torres and D. M. Guldi, *J. Am. Chem. Soc.*, 2010, 132, 16202–16211.
18 S. Schumann, R. A. Hatton and T. S. Jones, *J. Phys. Chem. C*, 2011, 115, 4916–4921.
19 M. E. Ragoussi, G. Katsukis, A. Roth, J. Malig, G. D. L. Torre, D. M. Guldi and T. Torres, *J. Am. Chem. Soc.*, 2014, 136, 4593–4598.
20 M. Scardamaglia, C. Struzzi, S. Lizzit, M. Dalmiglio, P. Lacovig, A. Baraldi, C. Mariani and M. G. Betti, *Langmuir*, 2013, 29, 10440–10447.
21 J. P. Mensing, T. Kerdcharoen, C. Sriprachuabwong, A. Wisitsoraat, D. Phokharatkul, T. Lomasa and A. Tuantranont, *J. Mater. Chem.*, 2012, 22, 17094–17099.
22 X. Q. Zhang, Y. Y. Feng, S. D. Tang and W. Feng, *Carbon*, 2010, 48, 211–216.
23 J. Malig, N. Jux, D. Kiessling, J. J. Cid, P. Vzquez, T. Torres and D. M. Guldi, *Angew. Chem. Int. Ed.*, 2011, 50, 3561–3565.
24 J. P. Zhong, Y. J. Fan, H. Wang, R. X. Wang, L. L. Fan, X. C. Shen and Z. J. Shi, *J. Power Sources*, 2013, 242, 208–215.
25 J. Borges and J. F. Mano, *Chem. Rev.*, 2014, 114, 8883−8942.
26 X. Y. Dong, L. Wang, D. Wang, C. Li and J. Jin, *Langmuir*, 2012, 28, 293–298.
27 Y. Zhang, F. F. Wen, Y. Jiang, L. Wang, C. H. Zhou and H. G. Wang, *Electrochim. Acta*, 2014, 115, 504–510.
28 T. T. Meng, Z. B. Zheng and K. Z. Wang, *Langmuir*, 2013, 29, 14314–14320.
29 L. L. Cui, T. Pu, Y. Liu and X. Q. He, *Electrochim. Acta*, 2013, 88, 559–564.
30 X. Zhang and Y. L. Chen, Inorg. *Chem. Commun.*, 2014, 39, 79–82.
31 A. Wojcik and P. V. Kamat, *ACS Nano*, 2010, 4, 6697–6706.
32 A. D. Adler, F. R. Longo, F. Kampas and J. Kim, *J. Inorg. Nucl. Chem.*, 1970, 32, 2443–2445.
33 H. L. Guo, X. F. Wang, Q. Y. Qian, F. B. Wang and X. H. Xia, *ACS Nano*, 2009, 3, 2653–2659.
34 K. Akatsuka, Y. Ebina, M. Muramatsu, T. Sato, H. Hester, D. Kumaresan, R. H. Schmehl, T. Sasaki and M. Haga, *Langmuir*, 2007, 23, 6730–6736.
35 H. J. Shin, K. K. Kim, A. Benayad, S. M. Yoon, H. K. Park, I. S. Jung, M. H. Jin, H. K. Jeong, J. M. Kim, J. Y. Choi, Y. H. Lee, *Adv. Funct. Mater.* 2009, 19, 1987–1992.
36 N. J. Bell, N. Y. Hau, A. Du, H. Coster, S. C. Smith, R. Amal, J. Phys. Chem. C 2011, 115, 6004-6009.



 